

A Study of Pedestrian Kinematics and Injury Outcomes Caused by a Traffic Accident with Respect to Pedestrian Anthropometry, Vehicle Shape, and Pre-Impact Conditions

Costin D. Untaroiu¹, Wansoo Pak¹, Yunzhu Meng¹, Berkan Guleyupoglu², Scott Gayzik²

¹Virginia Tech, Blacksburg, VA, USA, ²Wake Forest University, Winston-Salem, NC, USA

Abstract

Pedestrians represent one of the most vulnerable road users. In the U.S., pedestrian fatalities show an increasing trend from 11% of total traffic fatalities in 2007 to about 15% in 2015. The rapid advancement in finite element (FE) technology, material testing, and computational power promotes FE car-to-pedestrian collision (CPC) simulations as a very useful component in the vehicle design process (e.g., in designing deployable devices for pedestrian head protection). The objective of this study was to investigate the sensitivity of pedestrian kinematics and injury outcomes to pedestrian anthropometry, vehicle shape, and pre-impact conditions (e.g. vehicle speed, relative position of pedestrian to the vehicle). Three pedestrian FE adult models (5th percentile female-F05-PS, 50th percentile male-M50-PS and 95th percentile male-M95-PS) and a child model (6 year-old-6YO) developed and validated by our group were employed in this study. The geometry of these LS-DYNA[®] models were reconstructed from medical images of adult volunteer subjects or obtained from literature data (child model). Their material properties were assigned based on the Global Human Body Models Consortium (GHBMC) M50 occupant model (adult models) and from literature data (child model). Four simplified vehicle models corresponding to a family car, a roadster, a multi-purpose vehicle, and a sport utility vehicle were also used in this study. The geometric and front-end stiffness properties of these models were obtained based on current European car models. Then, CPC FE simulations were performed successfully in a Design-of-Experiments (DOE) fashion where the pedestrian anthropometry, vehicle shape, and pre-impact conditions were considered as variables. The pedestrian kinematics and the injuries were recorded at the end of each simulation (the head-to-vehicle contact). The results showed significant sensitivities of both pedestrian kinematics and injury outcomes which are not currently considered in pedestrian subsystem tests. For example, the head impact resultant velocity showed to increase for taller subjects (M95, M50), who impacted the vehicle into the windshield region compared to the shorter subjects (6YO, F05) who impacted the vehicle hoods. The results presented in this study could help both automotive manufacturers and government agencies to develop more pedestrian-friendly vehicles and to improve the current pedestrian safety regulations.

Introduction

Pedestrians represent one of the most vulnerable road users. According to the World Health Organization (WHO), the total number of fatalities recorded in traffic accidents is about 1.25 million each year worldwide [1]. In the U.S., pedestrian fatalities show an increasing trend from 11% of total traffic fatalities in 2007 to about 15% in 2015 [2].

During vehicle-pedestrian interaction, the pedestrian biomechanical and injury responses are influenced by various pre-impact variables. For example, significant differences were observed in terms of head injuries with respect to pedestrian anthropometry [3]. At the lower extremity level, more severe injuries were observed in heavier pedestrians possibly due to the greater inertia. In addition, traffic accident statistics analyses revealed higher pedestrian morbidity and mortality in accidents involved light trucks and vans compared to passenger cars [4, 5]. However, a correlation of pedestrian biomechanics and injuries relative to the pre-impact variables were not clearly defined. Therefore, the effect of these pre-impact variables should be investigated to improve the design of vehicle for pedestrian protection.

Recently, the rapid advancement in finite element (FE) technology, material testing, and computational power promotes FE car-to-pedestrian collision (CPC) simulations as a very useful component in pedestrian

protection. While the post mort human surrogate (PMHS) test provide the most biofidelic responses, this method is not suitable in design of experiment (DOE) study due to its high cost and unreproducible characteristics. Thus, various pedestrian FE models should be developed and validated to be used the DOE study. In this study, three adults and one child pedestrian FE models developed and validated previously were used to investigate the effect of the anthropometry, vehicle shape, and pre-impact conditions during CPC simulation.

Methods

Pedestrian FE models

The pedestrian FE models corresponding to a 6-years-old (6YO-PS), 5th percentile female (F05-PS), 50th percentile male (M50-PS), and 95th percentile male (M95-PS) anthropometries were developed and validated by our group [6-8]. These FE models were developed based on the geometry reconstructed from medical images of adult volunteer subjects (Table 1) or obtained from literature data (child model) [6]. The external anthropometry data and surface scans were integrated together for the generation of a non-uniform rational basis spline (NURBS) patchwork of the small female, average male, and large male outer surface in neutral standing posture. Surface data was symmetrized using methods described in literature [9]. A multi-modality protocol was used to acquire data in a pedestrian posture [10].

The mesh of the M50 model was mostly adapted from a 50th percentile male occupant (M50-O) model [11-16] and the F05 and M95 FE models were obtained by morphing a M50 model (Figure 1). The M50 model was morphed to target small female and large male geometries by using the outer surface and landmark data acquired from the small female and large male subjects using a radial basis interpolation function – thin plate spline approach [17]. Due to the morphing procedure, all modeling aspects including the number of nodes, elements, material types, and contact definitions are carried forward from the M50 model [18]. Only several elements were manually edited until their mesh quality was above the Global Human Body Model Consortium (GHBMC) quality thresholds [6]. The defined material properties of the pedestrian models were based on the GHBMC M50-O model.

Table 1. Data for the volunteer subjects

Subject	Age (years)	Height (cm)	Weight (kg)
Small female (F05)	24	149.9	48.1
Average male (M50)	26	174.9	78
Tall male (M95)	26	189.5	102.5

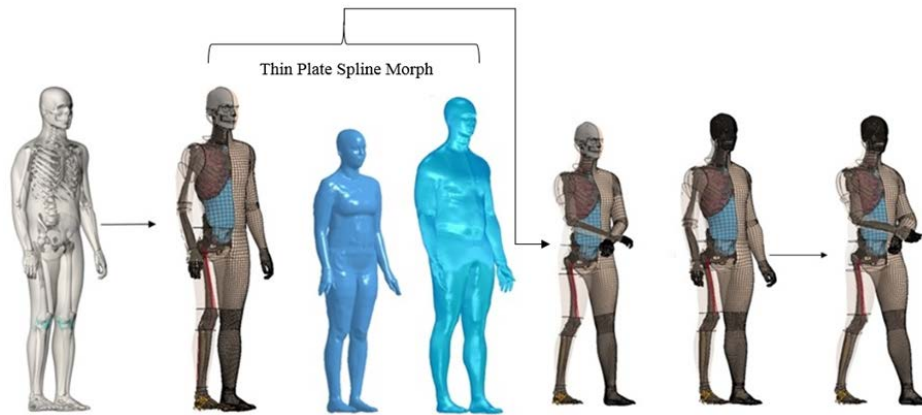


Figure 1. Schematic development procedure of adult pedestrian FE models

Vehicle FE models

Representative generic vehicle FE models of Family Cars (FCR), Roadsters (RDS), Multi-purpose vehicles and superminis (MPV), and Sport Utility Vehicle (SUV) [19] were used in this study. The geometry of these models was obtained by parametrization of current European cars corresponding to each vehicle category (Figure 2). The structure of each vehicle FE model consists of outer shell layer, an interface layer, and a foam layer resting on a rigid skeletal structure (the bottom layer) [19]. The structural properties of vehicle FE models were calibrated based on the corresponding average curves recorded in impactor FE simulations performed with validated FE models of current European cars.

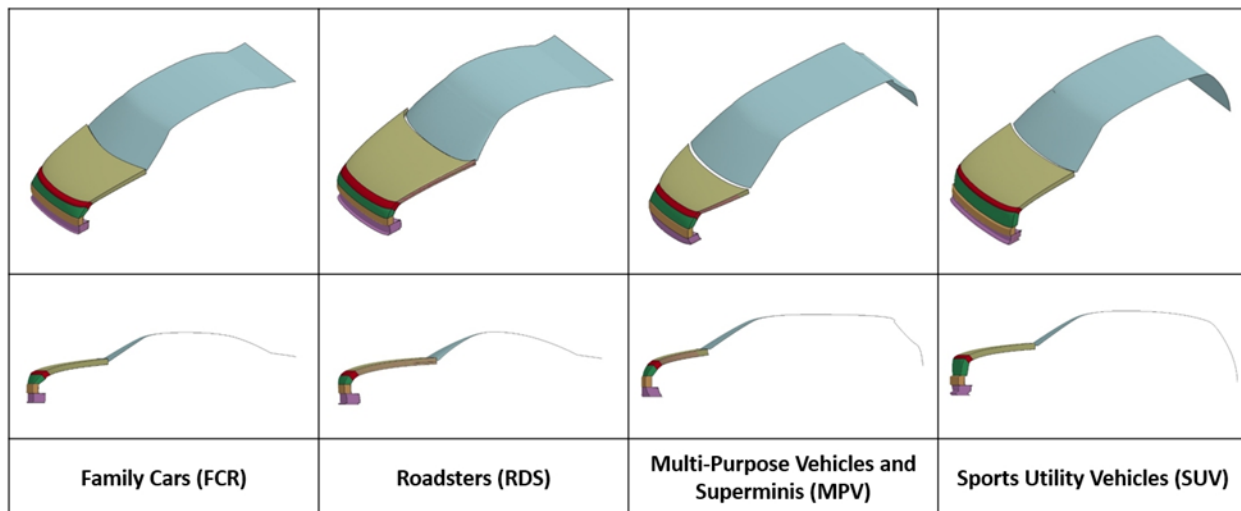


Figure 2. Schematic generic vehicle FE models

Car-to-pedestrian impact simulations

The pedestrian FE models (6YO-PS, F05-PS, M50-PS, M95-PS) were impacted laterally by the four generic vehicle FE models in order to study their kinematic responses with respect to the anthropometry, vehicle shape, and pre-impact conditions. The pedestrian FE models were positioned laterally at the centerline of the generic vehicle FE models (Figure 3). The posture of the FE model was set to mid-stance with the legs apart walking towards the vehicle centerline and the rearward leg being impacted first by the vehicle based on the pedestrian testing protocol of European New Car Assessment Program (Euro NCAP) [20]. Then, the vehicle

with 40 km/h initial velocity impacted to the pedestrian FE model. In addition, the velocity of head impact to the vehicle was calculated at the head CG. The static/dynamic friction coefficient were defined 0.3 for both the vehicle-pedestrian and the pedestrian-ground.

During simulation, the components of head impact velocity relative to the vehicle along the test directions (50°-child and 65°-adult from a plane parallel to the ground) used by the European Experimental Vehicle Committee (EEVC) headform test procedure were calculated (Table 2) [21]. In addition, the maximum Head Injury Criterion (HIC₁₅) values were calculated at the head CG (filtered SAE 180).

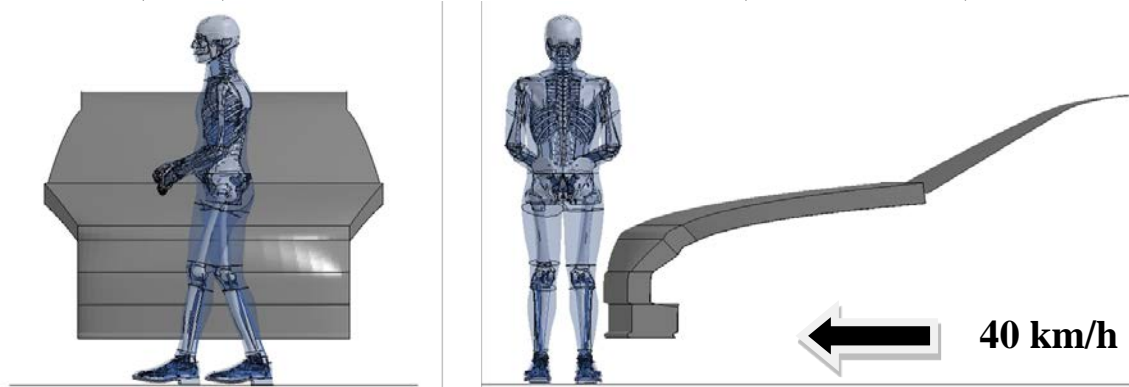


Figure 3. FE simulation setup: M50 pedestrian model with FCR vehicle

Results and Discussion

Overall, both the head impact time (HIT) and wrap around distance (WAD) showed an increase as the pedestrian model stature increased (Figure 4). In addition, pedestrian kinematics predicted by FE models showed significant differences in terms of vehicle shape (Figure 5). For example, the predicted F05’s WAD ranges from 1,352 mm (SUV) to 1,673 mm (RDS), while the predicted M50’s WAD ranges from 1,762 mm (SUV) to 2,125 mm (RDS).

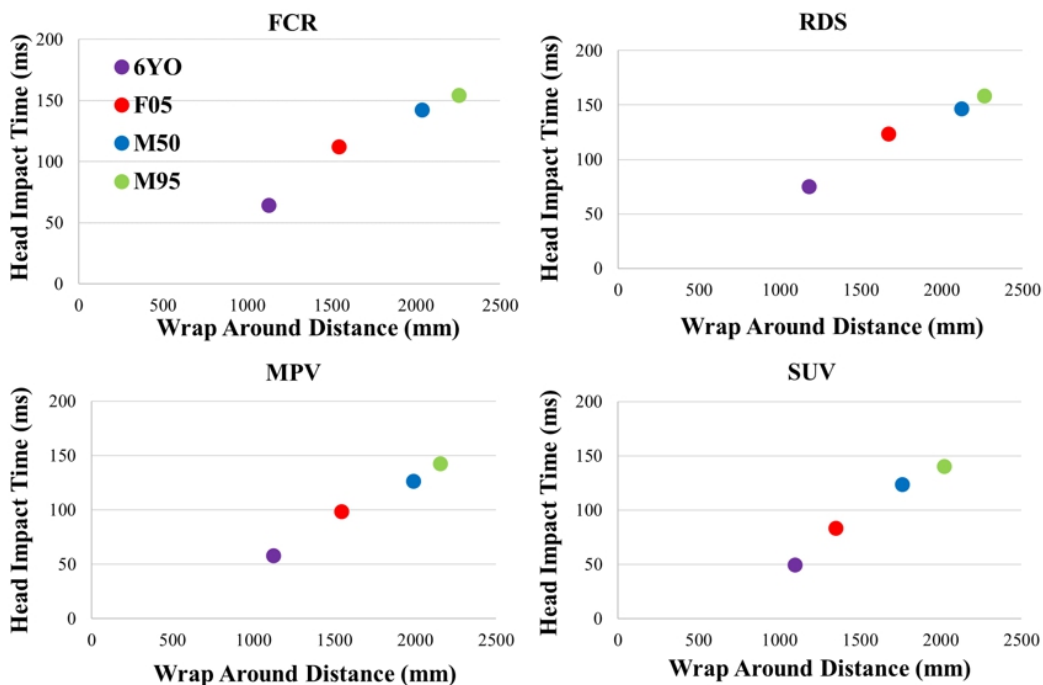


Figure 4. WAD vs. HIT with respect to the vehicle shape

The shortest values of HIT and WAD were observed during the SUV impacts and the largest values were observed during the RDS impacts. In terms of the head contact point to the vehicle, impacts to the hood were observed in the short stature models (6YO-PS and F05-PS) (Figure 5). The higher stature models (M50-PS and M95-PS) predicted mostly head contact to the windshield or to the SUV hood.

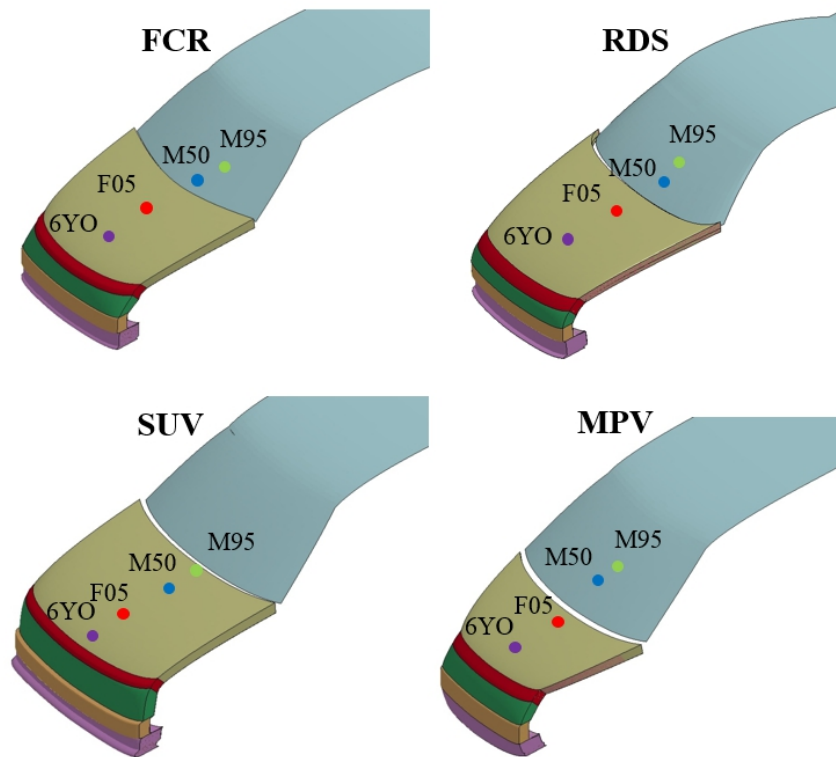


Figure 5. Head contact point to the vehicle

Mostly, the head impact velocity increase as the pedestrian’s height increases. No correlation between vehicle shape and head impact velocity was observed.

Table 2. Head impact velocity with respect to the vehicle types

	6YO		F05		M50		M95	
	50° velocity (m/s)	HIC ₁₅ (g)	65° velocity (m/s)	HIC ₁₅ (g)	65° velocity (m/s)	HIC ₁₅ (g)	65° velocity (m/s)	HIC ₁₅ (g)
FCR	5.47	68.6	7.98	177.8	7.66	563	6.0	662.4
RDS	4.62	237.6	7.80	442.4	6.73	813.2	4.95	205.8
MPV	5.70	76.5	8.62	144	6.08	642.6	2.63	731
SUV	4.82	88	10.46	306.3	6.66	116.3	8.86	107.7

The results presented by this preliminary study recommend the development of pedestrian active protection systems which can apply the best restraint system based on specific pre-impact conditions of a certain pedestrian accident. For example, the parameters of current and future pedestrian protection systems (e.g. pedestrian airbags, pop-up hoods, etc.[22-24]) could be selected from look-up tables based on the detected stature of pedestrian and its position relative to the car [25, 26]. We believe that the current pedestrian FE models and other future pedestrian FE models will be very useful in performing a huge number of CPC simulations for development of future adaptive pedestrian systems.

Acknowledgements

Funding for this study was provided by the Global Human Body Models Consortium (GHBMC). All findings and views reported in this manuscript are based on the opinions of the authors and do not necessarily represent the consensus or views of the funding organization.

References

- [1] WHO, 2016, "Road traffic injuries."
- [2] NHTSA, 2016, "2015 Motor Vehicle Crashes: Overview."
- [3] Zhang, G., Cao, L., Hu, J., and Yang, K. H., "A field data analysis of risk factors affecting the injury risks in vehicle-to-pedestrian crashes," Proc. Annals of Advances in Automotive Medicine/Annual Scientific Conference, Association for the Advancement of Automotive Medicine, p. 199.
- [4] Henary, B. Y., Crandall, J., Bhalla, K., Mock, C. N., and Roudsari, B. S., "Child and adult pedestrian impact: the influence of vehicle type on injury severity," Proc. Annual Proceedings/Association for the Advancement of Automotive Medicine, Association for the Advancement of Automotive Medicine, p. 105.
- [5] Lefler, D. E., and Gabler, H. C., 2001, "The emerging threat of light truck impacts with pedestrians," Rowan University.
- [6] Meng, Y., Pak, W., Guleyupoglu, B., Koya, B., Gayzik, F. S., and Untaroiu, C. D., 2017, "A finite element model of a six-year-old child for simulating pedestrian accidents," Accident Analysis & Prevention, 98, pp. 206-213.
- [7] Pak, W., and Untaroiu, C., "Development and Validation of a 95 th Percentile Male Pedestrian Finite Element Model."
- [8] Untaroiu, C. D., Pak, W., Meng, Y., Schap, J., Koya, B., and Gayzik, S., 2018, "A Finite Element Model of a Midsize Male for Simulating Pedestrian Accidents," Journal of biomechanical engineering, 140(1), p. 011003.
- [9] Gayzik, F., Moreno, D., Danelson, K., McNally, C., Klinich, K., and Stitzel, J. D., 2012, "External landmark, body surface, and volume data of a mid-sized male in seated and standing postures," Annals of biomedical engineering, 40(9), pp. 2019-2032.
- [10] Gayzik, F. S., Moreno, D. P., Geer, C. P., Wuertzer, S. D., Martin, R. S., and Stitzel, J. D., 2011, "Development of a full body CAD dataset for computational modeling: a multi-modality approach," Ann Biomed Eng, 39(10), pp. 2568-2583.
- [11] Beillas, P., and Bertet, F., 2012, "Performance of a 50th Percentile Abdominal Model for Impact: Effect of Size and Mass," J Biomechanics, 45(Suppl. 1), p. S83.
- [12] DeWit, J. A., and Cronin, D. S., 2012, "Cervical spine segment finite element model for traumatic injury prediction," J Mech Behav Biomed Mater, 10, pp. 138-150.
- [13] Shin, J., and Untaroiu, C. D., 2013, "Biomechanical and injury response of human foot and ankle under complex loading," J Biomech Eng, 135(10), p. 101008.
- [14] Shin, J., Yue, N., and Untaroiu, C. D., 2012, "A finite element model of the foot and ankle for automotive impact applications," Ann Biomed Eng, 40(12), pp. 2519-2531.
- [15] Untaroiu, C. D., Yue, N., and Shin, J., 2013, "A finite element model of the lower limb for simulating automotive impacts," Ann Biomed Eng, 41(3), pp. 513-526.
- [16] Mao, H., Zhang, L., Jiang, B., Genthikatti, V. V., Jin, X., Zhu, F., Makwana, R., Gill, A., Jandir, G., Singh, A., and Yang, K. H., 2013, "Development of a finite element human head model partially validated with thirty five experimental cases," J Biomech Eng, 135(11), p. 111002.
- [17] Vavalle, N. A., Schoell, S. L., Weaver, A. A., Stitzel, J. D., and Gayzik, F. S., 2014, "Application of radial basis function methods in the development of a 95th percentile male seated fea model," Stapp car crash journal, 58, p. 361.
- [18] Untaroiu, C. D., Pak, W., Meng, Y., Schap, J., Koya, B., and Gayzik, S., 2018, "A Finite Element Model of a Midsize Male for Simulating Pedestrian Accidents," J Biomech Eng, 140(1).
- [19] Klug, C., Feist, F., Raffler, M., Sinz, W., Petit, P., Ellway, J., and van Ratingen, M., "Development of a Procedure to Compare Kinematics of Human Body Models for Pedestrian Simulations," Proc. IRCOBI Conference Proceedings.
- [20] EURONCAP, 2017, "Pedestrian Testing Protocol,"file:///C:/Users/Student/Downloads/euro-ncap-pedestrian-testing-protocol-v84%20(2).pdf.
- [21] Janssen, E., "EEVC test methods to evaluate pedestrian protection afforded by passenger cars," Proc. Proceedings: International Technical Conference on the Enhanced Safety of Vehicles, National Highway Traffic Safety Administration, pp. 1212-1225.
- [22] Fredriksson, R., Shin, J., and Untaroiu, C. D., 2011, "Potential of Pedestrian Protection Systems-A Parameter Study Using Finite Element Models of Pedestrian Dummy and Generic Passenger Vehicles," Traffic Inj Prev, 12(4), pp. 398-411.
- [23] Fredriksson, R., Håland, Y., and Yang, J., 2001, Evaluation of a new pedestrian head injury protection system with a sensor in the bumper and lifting of the bonnet's rear part, Society of Automotive Engineers.
- [24] Untaroiu, C. D., Shin, J., Crandall, J. R., Fredriksson, R., Bostrom, O., Takahashi, Y., Akiyama, A., Okamoto, M., and Kikuchi, Y., 2010, "Development and validation of pedestrian sedan bucks using finite-element simulations: a numerical investigation of the influence of vehicle automatic braking on the kinematics of the pedestrian involved in vehicle collisions," Int J Crashworthines, 15(5), pp. 491-503.

[25] Adam, T., and Untaroiu, C. D., 2011, "Identification of occupant posture using a Bayesian classification methodology to reduce the risk of injury in a collision," *Transport Res C-Emer*, 19(6), pp. 1078-1094.

[26] Untaroiu, C. D., and Adam, T. J., 2013, "Performance-Based Classification of Occupant Posture to Reduce the Risk of Injury in a Collision," *Ieee T Intell Transp*, 14(2), pp. 565-573.